Applied Surface Science 346 (2015) 438–442

Contents lists available at ScienceDirect

Applied Surface Science

journal homepage: www.elsevier.com/locate/apsusc

Influence of coadsorbed H in CO dissociation and CH_n formation on Fe(1 0 0): A DFT study

S. Amaya-Roncancio [a], D.H. Linares [a,*], K. Sapag [a], M.I. Rojas [b]

[a] Departamento de Física, Instituto de Física Aplicada, Universidad Nacional de San Luis-CONICET, Ejército de Los Andes 950, D5700HHW San Luis, Argentina
[b] INFIQC-Departamento de Matemática y Física, Facultad de Ciencias Químicas, Ciudad Universitaria, 5000 Córdoba, Argentina

ARTICLE INFO

Article history:
Received 23 February 2015
Accepted 31 March 2015
Available online 7 April 2015

MSC:
00-01
99-00

Keywords:
DFT
Adsorption
Reaction
Catalysis
Fischer–Tropsch
Fe

ABSTRACT

Density functional theory (DFT) was employed to study the influence of coadsorbed hydrogen in CO dissociation and C hydrogenation on Fe(1 0 0). The formation of species CH_n ($n = 1, 2, 3$) from the reaction $CH_{n-1} + H$ as well as CO dissociation was analyzed in terms of hydrogen coverage. The active sites for the adsorption and reaction of each intermediate product on the catalytic surface and the reaction pathways of the products were determined. Mulliken population analysis was carried out to evaluate the charge transfer in the CH_n/Fe system. It was observed that carbon transfers charge in all cases, while the catalyst transfers charge principally in the adsorption of CH_2 and CH_3. To determine the effect of hydrogen on CO dissociation and CH_n formation, coverages of 0, 0.25, 0.50 and 0.75 monolayers of hydrogen were employed. The CO adsorption energy shows slight variations in the presence of hydrogen, while in CO dissociation the variations of the barriers were negligible. In CH_n adsorption, slight changes in the energies were observed. The reaction of C hydrogenation exhibited sensitivity to the presence of hydrogen, showing that CH and CH_2 formation were endothermic processes, while CH_3 formation showed an exothermic or endothermic behavior, depending on the final adsorption configuration.

1. Introduction

Fischer–Tropsch (FT) synthesis is the process by which CO and H_2 are converted into hydrocarbons through a catalytic surface as Fe, Co, Ru, Rh where the reaction takes place under specific conditions. This reaction is considered one of the most important discoveries related with heterogeneous catalysis and, although the practical and experimental interest in this synthesis has increased in the last years. The complete set of molecular details regarding the relation between the catalyst surface and the involved molecules is still unknown [1].

In general, FT synthesis could be visualized as a repeated step sequence where hydrogen atoms are bounded to the carbon and oxygen coming from CO dissociation produced on the surface. Furthermore, the hydrogen-rich atmosphere allows carbon atoms to react and form C—C bonds, and then long hydrocarbon chains are formed; while oxygen is eliminated from the surface, mainly as water [2].

FT synthesis can be described in the following steps: (a) adsorption of CO on the metal surface, (b) CO dissociation, (c) dissociative adsorption of H_2, (d) hydrogenation of carbon-containing species and oxygen, (e) C—C coupling and long chain formation. From the above steps, several questions arise, such as how the $H_2 + CO$ interaction on the surface happens, what the preferential sites are for the adsorbed species on the metal surface, what orientations adsorbed molecules prefer on the surface and how strong the energies involved are in each reaction and adsorption, among others.

Many authors have widely studied FT synthesis from the molecular point of view and have proposed several reaction mechanisms, such as those proposed by Anderson–Emmett [3], Sachtler–Biolen [4] and Pichler–Schulzs [5]. FT synthesis has been studied on several materials, principally on Co, Fe and Ru [6–9]. Although Ru has been found to be the more reactive, its high price and scarcity exclude it from industrial applications. In contrast, iron is inexpensive and abundant in nature which makes it attractive for use on an industrial scale, and hence, here lies our interest in using it as a catalyst.

From a practical point of view, computational analysis may help to clarify the understanding of the intermediate processes of the synthesis and also to determine the transition states and activation barriers. Generally, there is no one single way to set up FT reaction mechanisms, and we make use of previous results [10,11] to identify the active sites and the catalytic structure that favor the reactions. Following the mechanism explained by Hanz Schulz [12]

* Corresponding author. Tel.: +54 0266 4520300; fax: +54 0266 4447462.
E-mail address: dlinares@unsl.edu.ar (D.H. Linares).

http://dx.doi.org/10.1016/j.apsusc.2015.03.215
0169-4332/

and focusing on C_1 species (a single carbon), the main objective of the present work is to determine the effect of preadsorbed H coverage in the main elemental reactions of FT synthesis on Fe(1 0 0) surface. Thus, reactions such as CO adsorption, CO dissociation and CH_n (n = 1, 2, 3) formation were studied by means of density functional theory calculations.

2. Computational details

Calculations were performed using SIESTA code [13,14], and a localized basis set composed of double-Z plus polarization (DPZ) was used. The basis functions for the solution of the Kohn–Sham equations for the isolated pseudoatoms were numerical atomic orbitals (NAOs). Exchange and correlation effects were described using GGA with PBE functional [15]. The core electrons were replaced by norm conserving pseudopotentials [16] in their fully separable form [17]. In the pseudopotential description of the atoms, the following valence electronic states were considered: Fe $4s^2\ 3d^6$; C $2s^2\ 2p^2$; O $2s^2\ 2p^4$; H $1s^1$.

As SIESTA code employs NAOs, the program replaces some integrals in real space by sums in a finite three dimensional real space grid, using one single parameter to control the energy cutoff of the grid [13], which refers to the fineness of the grid, and was converged for all the systems studied here, finding an appropriate value of 250 Ry with an energy shift of 0.01 eV. To sample the Brillouin zone, Monkhorst–Pack method [18] was used employing k-point meshes of $4 \times 4 \times 1$ for the slab system. The supercell employed was tetragonal with x, y, z periodic boundary conditions. The Fe(1 0 0) surface was emulated by a $p(2 \times 2)$ 5-layer slab, with three bottom layers fixed and two top layers free to relax. To model the solid/vacuum interphase, a large unit cell vector in z direction was selected, so that the interaction between the system and their images became negligible. The vacuum region was 1.5 nm thick. The determination of the minimum energy path for the different reactions was undertaken using the Nudged Elastic Band (NEB) method [19,20] and the local minima were found through the conjugate gradient (CG) technique.

3. Results

At first, the adsorption sites and energies of the primary species involved in FT synthesis were analyzed. The adsorption energies of CH_n, CO and H on Fe(1 0 0) surface was calculated at hollow, bridge and atop sites. The adsorption energy of a molecule on a surface obeys the following equation,

$$E_{ads} = E_{cat} + E_{mol} - E_{mol+cat}, \quad (1)$$

where E_{ads} is the adsorption energy of the molecule on the surface, E_{cat} and E_{mol} are the catalyst and molecule energies in vacuum, respectively, and $E_{mol+cat}$ is the energy of the whole system. The adsorption energy of each molecule at each site is shown in Table 1. Only in the case of CO adsorption on Fe(1 0 0), the three kinds of adsorption sites were found; whereas only some of them were detected for the remaining species. The hollow constitute the preferential adsorption site for most species, due to greater coordination. In the particular case of CH3, due to their geometry, the adsorption on hollow is not possible and the following site of further coordination is the bridge one, which is the preferred site in this case. Moreover, the fact that bridge sites are more adsorptive than atop sites, and hollow sites more than bridge sites, is observed for all molecules except for CO, which shows a relatively low energy for bridge in relation to hollow and atop sites, in good agreement with Bromfield et al. [21]

The preferential adsorption sites of reactants as well as products were determined by the lowest energy (Fig. 1), the observed values being in good agreement with Van Santen et al. [22], and consistent with the results reported by Zhao et al. [23] and by Lo et al. [24].

Table 1
Adsorption energies of the adsorbates. The symbol * denotes that a stable minimum was not achieved.

Molecule	Adsorption energy (eV)			Distance (Å)		
	Atop	Bridge	Hollow	Atop	Bridge	Hollow
H	*	2.79	2.86	*	1.71	2.04
C	*	*	8.38	*	*	1.98
CH	*	*	7.55	*	*	2.06
CH_2	*	4.26	4.81	*	1.97	2.13
CH_3	2.24	2.35	*	1.98	2.18	*
CO	2.19	1.61	2.84	1.77	1.97	2.00

Hydrogen atoms adsorb at hollow and bridge sites and adsorption energies of 2.86 eV and 2.79 eV, respectively, with an energy difference of 0.07 eV. In the case of C and CH, stable minima were achieved only at hollow sites, which could be due to the high values of the adsorption energies (8.38 eV for C and 7.55 eV for CH).

For CH_2, the adsorption energy decreases more than thirty percent with respect to CH (from 7.55 eV to 4.81 eV), and the molecule adsorbs at hollow (4.81 eV) and bridge (4.26 eV) sites, with a difference of 0.55 eV between adsorption energies. Similarly, for CH_3 the adsorption energy decreases more than fifty percent with respect to CH_2 (from 4.26 eV to 2.35 eV), and the molecule adsorbs at bridge (2.35 eV) and atop (2.24 eV) sites, with a difference of 0.11 eV between adsorption energies. Adsorption sites can play an important role in adsorption, desorption and reaction of products. Particularly, bridge and atop sites are places where transitory species may capture H to form products and desorb [22,25–29].

To provide additional information about the interaction between atoms of molecules and surface for zero H coverage, a Mulliken population analysis was carried out on the CH_n/Fe system. It can be observed from Table 2 that in all cases the C atom transfers charge to the hydrogen atoms. In the first case (C/Fe), a slight amount of electrical charge is transferred to the surface but the adsorption energy is high (8.38 eV). When one hydrogen is bounded to the carbon (CH/Fe), an noticeable amount of electrical charge is transferred from the carbon to the hydrogen without a significant change of electrical charge in the catalyst, and the adsorption energy slightly decreases (7.55 eV). If another hydrogen is added (CH_2/Fe), the hydrogens and the carbon show a similar electric charge to the previous case, but the electrical charge of the catalyst and the adsorption energy change significantly (0.204 a.u.

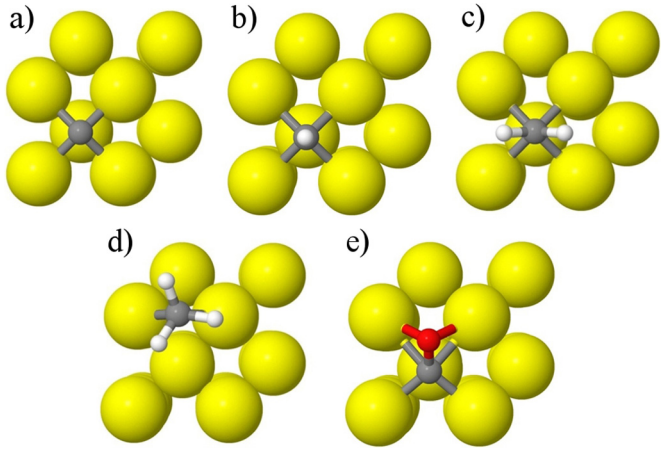

Fig. 1. Preferential adsorption sites on Fe(1 0 0) surface for reactants and intermediates of the FT synthesis. (a) C (hollow); (b) CH (hollow); (c) CH_2 (hollow); (d) CH_3 (bridge); (e) CO (hollow). Yellow: Fe; Gray: C; white: H; red O. Print version: Large: Fe, small: H; medium (light gray): C; medium (dark gray): O.

Table 2
Electric charge of adsorbate atoms and catalyst obtained from Mulliken analysis.

System	C/Fe	CH/Fe		CH_2/Fe			CH_3/Fe			
Atom	C	C	H1	C	H1	H2	C	H1	H2	H3
Q_{Atom} (a.u.)	0.054	0.223	−0.251	0.284	−0.244	−0.244	0.45	−0.209	−0.222	−0.224
$Q_{Catalyst}$ (a.u.)	−0.054	0.028		0.204			0.205			

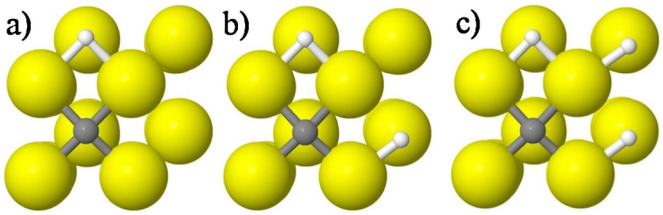

Fig. 2. Coadsorption of C + *n*H varying the coverage of H: (a) 0.25, (b) 0.50, and (c) 0.75 ML of H.

and 4.81 eV respectively), proving carbon as an electrical charge intermediary. In the last case (CH_3/Fe), the electrical charge of the hydrogen atoms and the catalyst is similar to the case of CH_2, but in this case it is the carbon that transfers the additional amount of electrical charge, weakening the carbon-surface bond (2.35 eV). Summarizing, the C-surface bond energy varies from 8.43 eV to 2.35 eV as *n* increases. After each hydrogenation step, the bond between the C and the surface is reduced (8.38 eV, 7.55 eV, 4.81 eV, 2.35 eV), while the distance to the surface increases (1.98, 2.06, 2.13, 2.18) which is in agreement with a decrease in the overlap between C and the surface, which facilitates the subsequent desorption of final products [27–29]. During hydrogenation steps, the catalyst not only provides support to the adsorbed species, but also transfers charge in order for the reaction to occurs.

3.1. Influence of hydrogen coverage on CH_n and CO adsorption

The variation of coadsorption energies of the adsorbate molecules were studied for 0, 0.25, 0.50 and 0.75 monolayers (ML) of H referring to hollow sites (Fig. 2). Ionic optimizations were carried out to find the minimal energy configurations of the coadsorbed species. The coadsorption energies found are shown in Table 3. The H coadsorption was performed as follow. To form 0.25 ML of H, an hydrogen atom was placed on one of the nearest hollow sites (Fig. 2(a). To form 0.5 ML of H, a second H atom was placed on the nearest hollow site (Fig. 2(b), and to form 0.75 ML of H coverage, a third hydrogen was placed on the second nearest hollow site (Fig. 2(c).

To elucidate the nature of lateral interactions arising from coadsorbed species, we proceeded as Liu et al.[30], by evaluating the change of adsorption energy (E_{ads}), where the increment or decrease in E_{ads} indicates the influence of lateral interactions between the adsorbate and the coadsorbed hydrogen atoms.

In the case of C, the larger change in the adsorption energy occurs at 0.75 ML of H coverage, having an increment of 1.1% in E_{ads} with respect to 0 ML. In the case of CH, we found a decrease of 1.4% on E_{ads}, 5.6% for CH_2, 11.7% for CO, and a negligible decrease for CH_3 (see Table 3)

Table 3
Adsorption, energy and preferred sites.

Adsorption energy (eV)				
Molecule	0 ML of H	0.25 ML of H	0.5 ML of H	0.75 ML of H
C	8.38	8.41	8.41	8.48
CH	7.54	7.48	7.60	7.44
CH_2	4.81	4.87	4.74	4.55
CH_3	2.35	2.35	2.35	2.34
CO	2.81	2.61	2.69	2.48

Table 4
Reaction barriers of CH_n formation in presence of 0, 0.25 and 0.50 ML of H coverage.

Reaction energy (eV)			
Reaction	E_{for}	E_{back}	ΔE
CO → C + O	1.05	1.69	−0.64
CO + H → C + O + H	1.04	1.69	−0.65
CO + 2H → C + O + 2H	1.00	1.66	−0.66

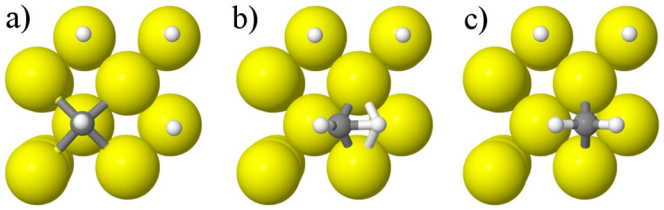

Fig. 3. Dissociation of CO for 0.50 ML of H. (a) Initial state (IS), (b) transition state (TS) and (c) final state (FS).

3.2. Influence of hydrogen coverage on CO dissociation and CH_n formation

To gain an insight into chain growth processes and to understand how lateral interactions modify the formation and dissociation barriers, we studied CH_n formation from CH_{n-1} and H, obtaining the reaction barriers for 0.25, 0.50 and 0.75 ML of H coverage (see Table 4). In general, there exist three steps to complete the reaction: the initial state (IS), transitions state (TS) and final state (FS), where E_{for} is the energy necessary to go from IS to TS and E_{back} is the energy needed to go from FS to TS. The configuration of IS, TS and FS are presented in Figs. 3–8. The difference between $E_{for} - E_{back}$ is called ΔE, which indicates if the reaction is endothermic ($\Delta E > 0$) or exothermic ($\Delta E < 0$). This can be observed in Table 4 for CO dissociation, and in Table 5 for CH_n formation.

3.2.1. CO dissociation

To understand the influence of H coverage on CO dissociation, direct dissociation was tested varying H coverage from 0 ML to 0.50 ML. As CO prefers to adsorb principally at hollow sites, this kind of sites were adopted as IS, as shown in Fig. 3(a). The adsorption energy and geometry configuration found for adsorbed CO are in good agreement with previous results reported by Sorescu et al.

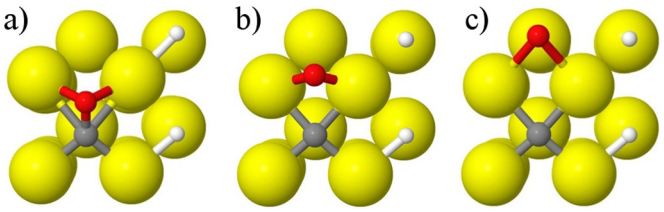

Fig. 4. Formation of CH for 0.75 ML of H. (a) Initial state (IS), (b) transition state (TS) and (c) final state (FS).

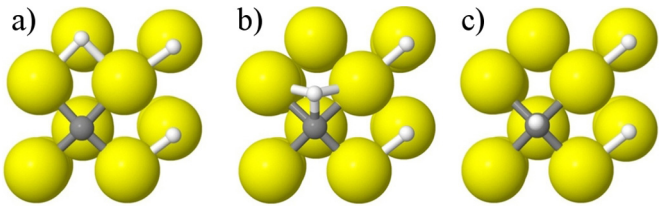

Fig. 5. Formation of CH_2 at hollow for 0.75 ML of H. (a) Initial state (IS), (b) transition state (TS) and (c) final state (FS).

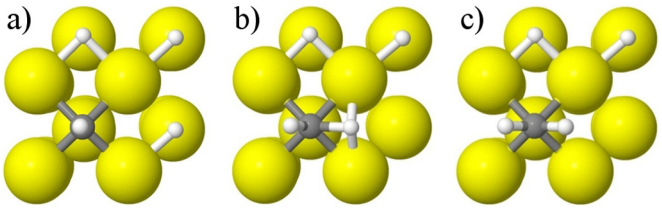

Fig. 6. Formation of CH_2 at bridge for 0.75 ML of H. (a) Initial state (IS), (b) transition state (TS) and (c) final state (FS).

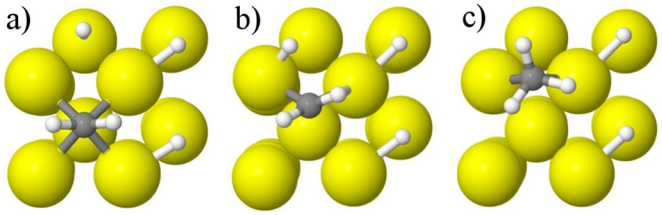

Fig. 7. Formation of CH_3 at hollow for 0.75 ML of H. (a) Initial state (IS), (b) transition state (TS) and (c) final state (FS).

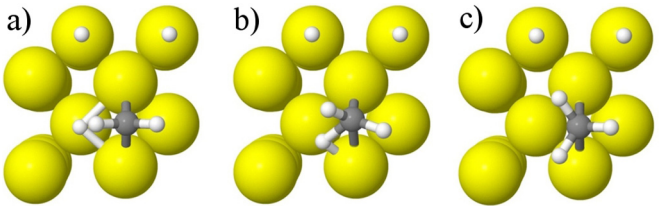

Fig. 8. Formation of CH_3 at bridge for 0.75 ML of H. (a) Initial state (IS), (b) transition state (TS) and (c) final state (FS).

Table 5
Reaction barriers of CH_n formation in presence of 0.25, 0.50 and 0.75 ML of hydrogen coverage.

Reaction energy (eV)				
Reaction	E_{for}	E_{back}	ΔE	Final state
$C + H \rightarrow CH$	0.83	0.60	0.22	Hollow
$C + 2H \rightarrow CH + H$	0.69	0.42	0.27	Hollow
$C + 3H \rightarrow CH + 2H$	0.71	0.38	0.33	Hollow
$CH + H \rightarrow CH_2$	0.82	0.23	0.59	Hollow
$CH + 2H \rightarrow CH_2 + H$	0.84	0.17	0.67	Hollow
$CH + 3H \rightarrow CH_2 + 2H$	0.91	0.17	0.74	Hollow
$CH + H \rightarrow CH_2$	1.00	0.62	0.38	Bridge
$CH + 2H \rightarrow CH_2 + H$	1.63	0.63	1.00	Bridge
$CH + 3H \rightarrow CH_2 + 2H$	1.07	0.87	0.20	Bridge
$CH_2 + H \rightarrow CH_3$	1.22	0.87	0.35	Hollow
$CH_2 + 2H \rightarrow CH_3 + H$	1.13	0.93	0.20	Hollow
$CH_2 + 3H \rightarrow CH_3 + 2H$	0.80	0.60	0.20	Hollow
$CH_2 + H \rightarrow CH_3$	0.49	1.61	−1.11	Bridge
$CH_2 + 2H \rightarrow CH_3 + H$	0.46	1.00	−0.54	Bridge
$CH_2 + 3H \rightarrow CH_3 + 2H$	0.49	2.00	−1.51	Bridge

[31]. The dissociation process was carried out via NEB method, choosing as FS a configuration with a C in the initial hollow site and an O in an adjacent hollow site, see Fig. 3(c). TS was found by the displacement of O through a bridge site, as shown in Fig. 3(b).

The values observed for E_{for} were 1.05 eV, 1.04 eV and 1.00 eV for 0, 0.25 and 0.50 ML of H coverage respectively, being 0.05 eV the largest change observed in the barrier. For the case of E_{back}, 1.69 eV to 0.00 and 0.25 ML of H coverage was found, and 1.66 eV for 0.50 ML of H coverage, showing that no significant changes were found in the barriers. All the dissociation reactions were exothermic (see Table 4), which is important to ensure a provision of carbon, necessary to construct long-chains of hydrocarbons.

3.2.2. CH formation

The final configuration for CH is on a hollow site. Due to the large difference between C and H adsorption energies, CH formation occurs when an H approaches an adsorbed C from an adjacent hollow sites (IS) (Fig. 4(a)). TS was found in a bridge site (Fig. 4(b)), while the final product (CH) is adsorbed on the hollow site initially occupied by the carbon (Fig. 4(c)). The forward barrier E_{for} decreases as the H coverage increases as shown in Table 5, where it can be seen that E_{for} takes the values 0.83, 0.69 and 0.71 eV to 0.25, 0.50 and 0.75 H ML respectively, showing a decrease of 0.14 eV and 0.12 eV for 0.50 and 0.75 H ML. Hence, lateral interactions facilitate the reaction. Similarly to E_{for}, E_{back} present a decrease of 0.18 eV and 0.22 eV for 0.50 and 0.75 H ML (see Table 5), showing that CH formation and dissociation is sensitive to H coverage [32,31]. As indicated by $\Delta E > 0$ (Table 5) the reaction is endothermic, and the results are in agreement with Zhao and Lo [23,24].

3.2.3. CH_2 formation

From the fact that CH_2 adsorbs at hollow as well as bridge sites, two paths are possible to form the product of the reaction. At first, as the previous case (CH formation), adjacent hollow sites are taken as the first initial configuration for the reaction (Fig. 5(a)). The adsorption energies of the reactants (CH and H) are quite different, hence FS is a CH_2 molecule adsorbed at the hollow site originally occupied by a CH molecule (Fig. 5(c)). The reaction begins when hydrogen moves toward the carbon, reaching TS at the bridge site located between the initial hollow sites (Fig 5(b)). It was observed that E_{for} was 0.82 eV for 0.25 H ML, being this value greater than the reported by Lo and Zhao; and E_{back} is in agreement with the value reported by John M. H. Lo but lower than the value reported by Zhao [24,23]. With the change of H coverage from 0.25 to 0.75 ML, E_{for} changes from 0.82 to 0.91 eV, but E_{back} decreases from 0.23 eV to 0.17 eV (see Table 5). Hence, lateral interactions would make CH_2 formation difficult at hollow when H coverage increases, making the reaction more endothermic [31]. For the second path FS consists of a CH_2 adsorbed in the bridge site, Fig 6(c). This FS is between the adjacent hollow sites in which CH and H are initially adsorbed (IS) (see Fig. 6(a)). TS takes place when CH and H approach to a bridge site to form CH_2 (see Fig. 6(b)). For 0.50 H ML, the forward barrier increases from 1.0 eV to 1.6 eV with no significant change in the backward barrier, which difficult the product formation. In the case of 0.75 H ML, the forward barrier has a slight change while the backward barrier increases from 0.62 eV to 0.87 eV, favoring CH_2 formation at bridge sites (see Table 5).

3.2.4. CH_3 formation

CH_3 adsorbs at bridge and atop sites, and two formation paths were possible to achieve. In the first path, adsorbed H and CH_2 at adjacent hollow sites approach each other and form CH_3 at the bridge site (see Fig. 7). Similar to the analysis of CH and CH_2 pathways, E_{for} is 1.22 eV, and E_{back} is 0.87 eV for 0.25 ML of H coverage. For 0.50 ML and 0.75 ML of H coverage, E_{for} is 1.13 eV and 0.80 eV respectively, these values being lower than the case of 0.25 ML of

H. In the case of E_{back}, the energy values are 0.87 eV, 0.93 eV and 0.60 eV, for 0.25 ML, 0.50 ML and 0.75 ML H coverage respectively. Here, ΔE shows an endothermic nature of the reaction, indicating that H coadsorption makes it difficult to reach the final state (see Table 5).

An exothermic path was found in CH_3 formation, when CH_2 was initially adsorbed at bridge site and the H atom approached CH_2 from a nearest hollow site (Fig. 8). The forward barrier did not show major variations for the H coverages studied. The coadsorption of H changed E_{back}, and the higher value (about 2 eV) was found at the maximum H coverage. However, no regular behavior was found for 0.50 H ML, where the minimum value for E_{back} was found to be 1.00 eV, as can be seen in Table 5.

4. Conclusions

DFT calculation using GGA-PBE exchange correlation functional was used to determine the effect of H coverage on the adsorption and dissociation of CO, as well as CH_n adsorption and formation on Fe(1 0 0) surface. The preferential adsorption site of H, CO, C, CH and CH_2 was hollow, and bridge sites for CH_3. For H, CO and CH_2, the adsorption was also possible in bridges. Finally, for CO and CH_3, adsorption was achieved in atop site.

The Mulliken analysis showed that in all cases, the carbon transfers charge. In the case of C/Fe, the charge transfer was not significant, and for CH/Fe, the major part of charge transferred to H came from C. In CH_2/Fe, the surface transfers a significant amount of charge taken for H atoms, showing a behavior of reductive agent. In CH_3/Fe, the charge taken by H atoms derived principally from C, and the catalyst transfers about the same charge as in CH_2/Fe case.

The influence of H on the adsorption energies of C, CO, CH_n was observed, where E_{ads} generally exhibits slight variations in all cases. On a clean Fe(1 0 0) surface, CO is highly activated and has a dissociation barrier of 1.05 eV and an association barrier of 1.69 eV. This dissociation presents an exothermic ΔE of 0.64 eV. Under H co-adsorption, CO activation has presented a negligible change, being 0.05 eV the major decrease in the energetic barrier and the maximum change is not more than 5%.

CH formation has a barrier of 0.83 eV for 0.25 H ML. With respect to 0.25 H ML, the barrier decreases about 17% for 0.50 H ML and 14.5% for 0.75 H ML, showing some sensitivity to the presence of H. On the other hand, the presence of H affects the CH dissociation barrier, reducing it about 30% for 0.50 H ML, and 37% for 0.50 H ML.

As regards the 0.25 H ML case, the formation barrier of CH_2 at hollow shows an increase of 11% for 0.75 H ML. However, for 0.50 H ML, the increase was just about 2.4%. Additionally, for E_{back} there exists a decrease of 26% for 0.50 and 0.75 H ML. It can be concluded that the presence of H atoms increases the barrier formation, but it decreases the dissociation barrier. The formation of CH_2 at bridge is endothermic, as previously stated. For 0.25 and 0.75 H ML, the forward barrier has values around 1.00 eV, and 1.63 eV for 0.50 H ML. For E_{back}, the barrier has an increase from 0.62 eV to 0.87 eV, with an increment of H coverage. In comparison with CH_2 at hollow, CH_2 at bridge shows more stable final states.

Finally, CH_3 at hollow shows an endothermic reaction, with a decrease of the formation barrier from 1.22 eV to 0.80 eV. E_{back} presents 0.87 eV, 0.93 eV and 0.60 eV for 0.25, 0.50 and 0.75 H Ml respectively. However, the formation of CH_3 at bridge presents an exothermic nature, having a small formation barrier of 0.5 eV, and a different dissociation barrier related to the presence of coadsorbed H.

Acknowledgements

This work was financially supported by UNSL, ANPCyT and CONICET (Argentina). The authors would also like to thank members of GAECI for their services and help.

References

[1] M. Corral Valero, P. Raybaud, Catal. Lett. 143 (2013) 1.
[2] X.-Q. Gong, R. Raval, P. Hu, Surf. Sci. 562 (2004) 247.
[3] W.K. Hall, R.J. Kokes, P.H. Emmett, J. Am. Chem. Soc. 82 (1960) 1027, http://dx.doi.org/10.1021/ja01490a005
[4] P. Biloen, W. Sachtler, Academic Press (1981), 165–216.
[5] H. Schulz, Appl. Catal. A: Gen. 186 (1999) 3.
[6] E. Iglesia, Appl. Catal. A: Gen. 161 (1997) 59.
[7] A.Y. Khodakov, W. Chu, P. Fongarland, Chem. Rev. 107 (2007) 1692, http://dx.doi.org/10.1021/cr050972v, pMID: 17488058.
[8] T. Riedel, M. Claeys, H. Schulz, G. Schaub, S.-S. Nam, K.-W. Jun, M.-J. Choi, G. Kishan, K.-W. Lee, Appl. Catal. A: Gen. 186 (1999) 201.
[9] M. Trpanier, A. Tavasoli, A.K. Dalai, N. Abatzoglou, Appl. Catal. A: Gen. 353 (2009) 193.
[10] J. Cheng, P. Hu, P. Ellis, S. French, G. Kelly, C.M. Lok, J. Phys. Chem. C 112 (2008) 6082.
[11] S. Shetty, R.A. van Santen, P.A. Stevens, S. Raman, J. Mol. Catal. A: Chem. 330 (2010) 73.
[12] H. Schulz, Appl. Catal. A: Gen. 186 (1999) 3.
[13] P. Ordejón, E. Artacho, Soler, Phys. Rev. B – Condens. Matter Mater. Phys. 53 (1996) R10441, cited by (since 1996):1477.
[14] J.M. Soler, E. Artacho, J.D. Gale, A. Garca, J. Junquera, P. Ordejn, D. Snchez-Portal, J. Phys.: Condens. Matter 14 (2002) 2745.
[15] J.P. Perdew, K. Burke, M. Ernzerhof, Phys. Rev. Lett. 77 (1996) 3865.
[16] N. Troullier, J.L. Martins, Phys. Rev. B 43 (1991) 1993.
[17] L. Kleinman, D.M. Bylander, Phys. Rev. Lett. 48 (1982) 1425.
[18] H.J. Monkhorst, J.D. Pack, Phys. Rev. B 13 (1976) 5188.
[19] G. Henkelman, B.P. Uberuaga, H. Jonsson, J. Chem. Phys. 113 (2000) 9901.
[20] G. Henkelman, H. Jonsson, J. Chem. Phys. 113 (2000) 9978.
[21] T.C. Bromfield, D. Curulla Ferr, J.W. Niemantsverdriet, ChemPhysChem 6 (2005) 254.
[22] R.A. Van Santen, I.M. Ciobîc, E. Van Steen, M.M. Ghouri, Adv. Catal. 54 (2011) 127.
[23] X.-h. Zhao, Y.-w. Li, J.-g. Wang, C.-f. Huo, J. Fuel Chem. Technol. 39 (2011) 956.
[24] J. Lo, T. Ziegler, J. Phys. Chem. C 111 (2007) 11012.
[25] M. Ozbek, I. Onal, R. van Santen, J. Catal. 284 (2011) 230.
[26] T. Zhu, P.W. Van Grootel, I.A.W. Filot, S.G. Sun, R.A. Van Santen, E.J.M. Hensen, J. Catal. 297 (2013) 227.
[27] Z. Zuo, W. Huang, P. Han, Z. Li, Appl. Surf. Sci. 256 (2010) 5929.
[28] I.M. Ciobica, R.A. van Santen, J. Phys. Chem. B 106 (2002) 6200.
[29] R. van Santen, A. Runstraat, R. Gelten, in: G. Froment, K. Waugh (Eds.), Studies in Surface Science and Catalysis, Proceedings of the International Symposium, vol. 109, Elsevier, 1997, pp. 61–77.
[30] H. Liu, R. Yan, R. Zhang, B. Wang, K. Xie, J. Nat. Gas Chem. 20 (2011) 611.
[31] D.C. Sorescu, Surf. Sci. 605 (2011) 401.
[32] F. Besenbacher, L.P. Nielsen, P. Sprunger, The Chemical Physics of Solid Surfaces, vol. 8, Elsevier, 1997, pp. 207–257.